Time-dependent phenomena in phase-separated electron-doped manganites

D. Niebieskikwiat,[1,2] J. Tao,[3,*] J. M. Zuo,[3] and M. B. Salamon[1,†]

[1]*Department of Physics and Frederick Seitz Materials Research Laboratory, University of Illinois at Urbana-Champaign, Urbana, Illinois 61801, USA*

[2]*Colegio de Ciencias e Ingeniería, Universidad San Francisco de Quito, Quito, Ecuador*

[3]*Department of Materials Science and Engineering and Frederick Seitz Materials Research Laboratory, University of Illinois at Urbana-Champaign, Urbana, Illinois 61801, USA*

(Received 17 October 2007; revised manuscript received 11 June 2008; published 31 July 2008)

We present time-dependent behavior of the transport and magnetic properties in electron-doped manganites. The relaxation of the electrical resistivity (ρ) shows a clear correlation with the microscopic properties of the samples observed through transmission electron microscopy. Two different relaxation mechanisms could be distinguished in $La_{0.23}Ca_{0.77}MnO_3$. One of them was found to be common to different electron-doped manganites and is associated with a defective formation of the charge-order (CO) phase. The second one is the result of the coexistence of the CO phase with a secondary charge-disordered (CD) phase. In this case, a low-temperature boundary between static and dynamic phase-separation regimes is determined by the appearance of a small ferromagnetic moment associated with the CD volume. These results show that kinematic constraints and magnetoelastic interactions are key ingredients for a proper understanding of phase-separated manganites.

DOI: 10.1103/PhysRevB.78.014434 PACS number(s): 75.47.Lx, 61.20.Lc, 75.60.Ch, 72.80.Ga

Ferromagnetic/antiferromagnetic (FM/AFM) phase separation (PS) in the manganese perovskites has attracted considerable attention in recent years due to the enormous magnetoresistance (MR) inherent to this state.[1] FM-metallic and AFM-insulating phases compete for the volume of the material, resulting in two-phase coexistence. The application of a magnetic field tilts the balance toward the FM state, inducing the growth of the metallic domains and a large drop of the electrical resistivity.

Despite the extensive experimental and theoretical research work done on phase-separated manganites,[1] new experimental results evidence the need of a deeper understanding of the PS phenomenon.[2–9] Disorder-induced PS (Refs. 1 and 10) and charge segregation[1,11] dominate the landscape of theoretical models and seem to explain the occurrence of PS quite successfully. However, even though dynamic effects have been often observed,[2,8,9] these are not directly included in the usual theories of PS. Moreover, an alternative scenario where PS is the result of the inability of the system to reach the real ground state because of kinematic restrictions cannot be discarded.[2,3,8,12] In a recent work,[2] we have shown that the $La_{0.23}Ca_{0.77}MnO_3$ manganite presents a phase-separated state, where charge-ordered (CO) orthorhombic and charge-disordered (CD) monoclinic domains coexist.[13] In this system, elastic effects were argued to be at the origin of the dynamic nature of the observed PS. A particular lamellar pattern has been observed, where the CD phase appears as sheets embedded in the CO matrix, suggesting that strain fields at the interfaces play an important role. Indeed, strain effects have been suggested to influence the physical properties of a variety of manganite compounds presenting phase separation.[2–4,12,14–17]

In this work we complement our previous paper on $La_{0.23}Ca_{0.77}MnO_3$ (Ref. 2) by studying the temporal evolution of the magnetic and transport properties in this and similar compounds. We report the presence of two competing mechanisms that contribute to the relaxation of the electrical resistivity. One of them is intrinsic to the CO phase and can also be observed in $La_{1/3}Ca_{2/3}MnO_3$ and $Pr_{1/3}Ca_{2/3}MnO_3$ (PCMO), where the CD phase is not present. The second mechanism, related to the motion of the domain boundaries separating the CO and CD domains, is strongly influenced by the magnetic state of the material. The competition between these two mechanisms can give some peculiar time evolution of the resistivity, decreasing in time after an initial increase.

$La_{1-x}Ca_xMnO_3$ and $Pr_{1-x}Ca_xMnO_3$ polycrystalline samples were prepared by the nitrate decomposition route,[18] starting from high-purity La_2O_3, Pr_6O_{11}, $CaCO_3$, and MnO. The final sintering process was performed at 1500 °C during 24 h. Electrical resistivity (ρ) data were obtained by the usual four-probe method in a Quantum Design physical property measurement system (PPMS) for temperatures T between 30 and 300 K. The resistivity as a function of time (t) was recorded after cooling the samples from 300 K at 4 K/min, followed by a careful stabilization at the measuring temperature within ± 2 mK. Magnetization (M) measurements were carried out in a superconducting quantum interference device (SQUID) magnetometer, with an applied field $H=100$ Oe. The transmission electron microscopy (TEM) experiments were performed in a JEOL 2010F (200 kV) microscope under the experimental conditions previously described.[17]

In Fig. 1 we show the very dissimilar temporal evolution of the resistivity for the $La_{0.23}Ca_{0.77}MnO_3$ and $La_{1/3}Ca_{2/3}MnO_3$ samples, measured at $T=90$ K during 24 h. On the contrary, the temperature dependence of ρ is quite similar in both samples: on cooling, the resistivity exhibits a pronounced increase at the CO transition (at $T_{CO}\approx 220$ and 278 K for $x=0.77$ and 2/3, respectively), followed by a strong insulating behavior at lower temperatures (see inset of Fig. 1). This demonstrates that the opposite slopes in $\rho(t)$ cannot be attributed to a systematic temperature drift during the experiment (both samples were measured simultaneously in the same run). The different time dependences indicate

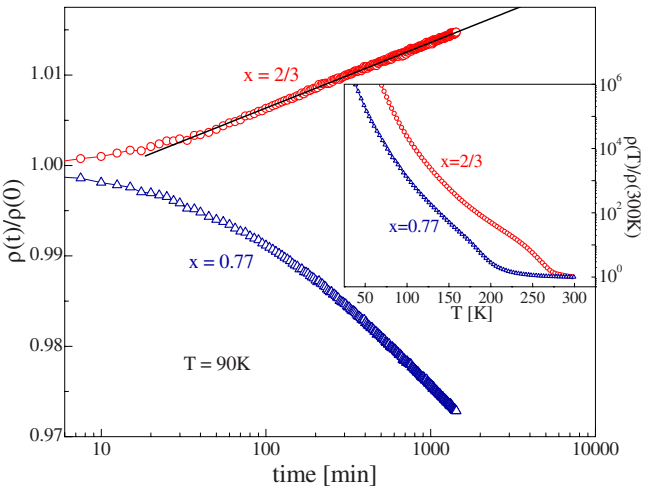

FIG. 1. (Color online) Resistivity as a function of time at $T=90$ K for the $La_{1-x}Ca_xMnO_3$ samples. The solid line shows the logarithmic behavior for $x=2/3$. Inset: temperature dependence of ρ for the same samples.

deep differences in the physical properties of the two doping levels.

In Fig. 2 we show the logarithmic relaxation rate of the resistivity, $S=d(\log \rho)/d(\log t)$, as a function of temperature for both samples (S was calculated in the timeframe $10 \text{ min} < t < 20 \text{ min}$). The dynamic behavior of the studied samples is summarized in this plot, where the difference between $x=2/3$ and 0.77 in $La_{1-x}Ca_xMnO_3$ becomes even more evident. For $x=0.77$, negative values of S are only

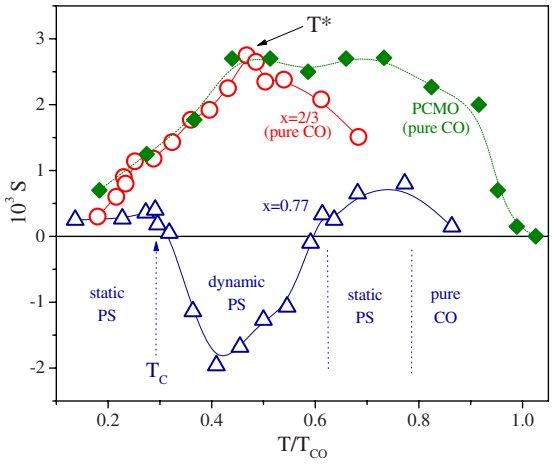

FIG. 2. (Color online) Temperature dependence of the logarithmic relaxation rate of the resistivity, $S=d(\log \rho)/d(\log t)$, for the $La_{1-x}Ca_xMnO_3$ samples (open triangles for $x=0.77$ and open circles for $x=2/3$). We also include $S(T)$ for $Pr_{1/3}Ca_{2/3}MnO_3$ (labeled as PCMO, solid diamonds). The labels "static PS" and "dynamic PS" refer to the different relaxation regimes for the sample $x=0.77$ in its phase-separated state, while "pure CO" indicates a pure charge-order phase. T_C indicates the low-temperature boundary between the static and dynamic PS regimes for $x=0.77$. This temperature coincides with the appearance of a small FM moment in the sample. Below T^* the positive relaxation rate for $La_{1/3}Ca_{2/3}MnO_3$ and $Pr_{1/3}Ca_{2/3}MnO_3$ rapidly decreases, indicating the freezing of the motion of defects within the CO phase.

found in the range $64 \text{ K} < T < 135 \text{ K}$ ($0.3 \leq T/T_{CO} \leq 0.6$). Outside this interval S is always positive. We have previously shown[2] that, in this sample, the decrease of ρ with time at intermediate temperatures is induced by the expansion of a secondary (less resistive) CD phase that appears immersed within the predominant CO volume. This regime is labeled as "dynamic PS" in Fig. 2. Even though this secondary phase appears at higher temperatures (at $T_{CD} \sim 170 \text{ K} \sim 0.77 T_{CO}$), the phase-separated state remains static for T above 135 K ("static PS" regime for $0.6 < T/T_{CO} < 0.77$ in Fig. 2).[2] Notably, in this static PS regime where the CO and CD domains remain static, the negative relaxation rate is lost and the resistivity for $x=0.77$ increases with time ($S>0$). In agreement with this picture, the sample with $x=2/3$, where the secondary CD phase was not observed and the volume is purely charge ordered,[17] does not show a negative relaxation rate. On the contrary, for $x=2/3$ the resistivity increases with time over the whole temperature range below T_{CO} (typically with a logarithmic time dependence, $\rho \sim \log t$). At this point we must note that in some cases a minor amount of monoclinic phase (a few percent) has been observed in $La_{1/3}Ca_{2/3}MnO_3$,[19–21] while in some other cases this minority phase was not detected.[17,22,23] Considering that this monoclinic phase starts to show up at doping levels x right above 2/3,[24] it is not surprising to have such a discrepancy, which can be readily attributed to different sample quality, stoichiometry, and preparation routes, as it was previously suggested.[21] In our $x=2/3$ sample we did not find evidence of a monoclinic phase. Nevertheless, even if there is a small amount of CD phase, its insignificant volume fraction would not affect the physical properties or the conclusions of our work.

We conclude that positive values of S are not related to the CO/CD coexistence but are a property of the charge-ordered phase itself. This means that either in the static PS regime or in the pure CO phase the positive relaxation rate is related to the same physical phenomenon, i.e., the resistivity of the CO phase increases with time. Even more remarkably, the evolution of ρ has a clear correlation with the microscopic properties of the CO phase, as demonstrated by the TEM experiment shown in Fig. 3 for $x=0.77$. In this figure we plot the temporal evolution of the peak intensity of the CO superlattice reflections (SLRs) around the (204) fundamental peak (these satellite reflections appear in electron-diffraction patterns as a consequence of the lattice modulation typical of the CO phase).[2] These data were collected at $T=176$ K ($T/T_{CO}=0.8$), where ρ increases with time (see Fig. 2 and inset of Fig. 3). As observed, the intensity of the CO superlattice peaks also increases over the same time interval. The width of these peaks is comparable to the resolution limits of our TEM experiments. Therefore, from the electron-diffraction patterns we are not able to determine whether the average correlation length of the CO phase also changes with time. Our TEM observations, however, clearly indicate that after cooling the sample below T_{CO} some non-CO volume is still present and slowly transforms into the CO state as the time evolves. Previously,[2] we attributed this phenomenon to the existence of small mobile defects in the CO phase of the $La_{0.23}Ca_{0.77}MnO_3$ compound, which also show up in magnetization measurements as a difference be-

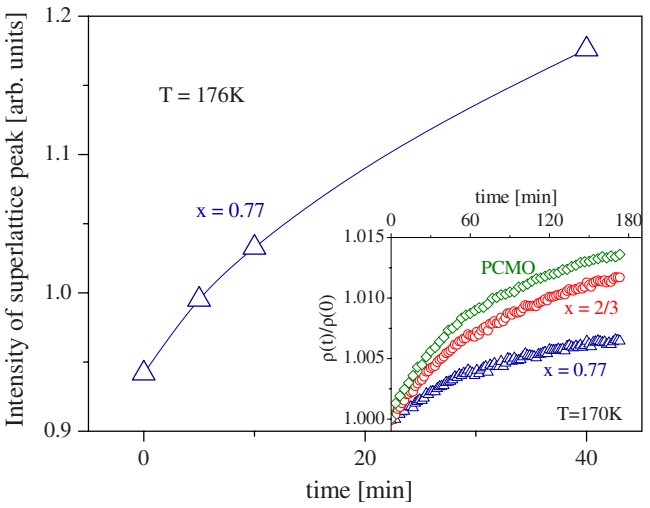

FIG. 3. (Color online) From electron-diffraction experiments we obtained the charge-order superlattice reflections (SLRs) around the (204) fundamental spot. This figure presents the time dependence of the peak intensity of these SLRs for the $La_{0.23}Ca_{0.77}MnO_3$ sample ($x=0.77$) at $T=176$ K. The inset shows that at a similar temperature (170 K) the resistivity also increases with time, as it does in $La_{1/3}Ca_{2/3}MnO_3$ ($x=2/3$) and $Pr_{1/3}Ca_{2/3}MnO_3$ (PCMO).

tween the field-cooling (FC) and zero-field-cooling (ZFC) data. Due to the charge-localized nature of the CO phase, the presence of defects provides a mechanism for charge transport instead of acting as scattering centers as it would be in conducting materials. Therefore, as these defects are expelled out of the CO volume the resistivity increases with time.

In the closely related $Pr_{1/3}Ca_{2/3}MnO_3$ a time-increasing resistivity is also observed at all temperatures below $T_{CO} \approx 273$ K (see, for example, the curve labeled as PCMO in the inset of Fig. 3). In fact, the dynamic properties of PCMO and $La_{1/3}Ca_{2/3}MnO_3$ turn out to be qualitatively the same, i.e., they show similar $S(T)$ curves. Also, TEM experiments in PCMO show the CO phase alone, with no evidence of CD-monoclinic domains, exactly as in $La_{1/3}Ca_{2/3}MnO_3$. Moreover, in the PCMO compound we have recently unveiled the presence of nanoscopic FM droplets embedded within the CO-AFM background,[6] which give rise to a FC-ZFC irreversibility and exchange-bias behavior (a shift of the M vs H curves after cooling the sample with an applied magnetic field). These two phenomena had been verified to occur in $La_{1/3}Ca_{2/3}MnO_3$ as well. Finally, we mention that a small positive relaxation rate of the resistivity was also observed in $La_{0.20}Ca_{0.80}MnO_3$. All these similarities give further support to the picture of a defective CO state, universal to these electron-doped manganites. Likely, these nanoscopic defects are formed at the CO transition due to the disordered growth of the CO volume. As evidenced in previous TEM experiments,[17] the transition at $T_{CO} \approx 278$ K in $La_{1/3}Ca_{2/3}MnO_3$ signals the appearance of charge-ordered clusters within the nonordered volume. As the temperature decreases the CO clusters rapidly grow and percolate, leaving small structural defects trapped within the distorted CO matrix.

Presumably, as the temperature decreases below T_{CO} the defects become more unstable inside the CO matrix, favoring a faster escape from the CO volume with a consequent increase in the relaxation rate (see S vs T for $x=2/3$ and PCMO in Fig. 2). However, in both $La_{1/3}Ca_{2/3}MnO_3$ and $Pr_{1/3}Ca_{2/3}MnO_3$ the maximum of S at intermediate temperatures and its rapid decrease below $T^* \sim 0.5T_{CO}$ (see Fig. 2) indicates that at low temperatures the thermal energy is not enough to allow the motion of the defects. While other dynamical processes in manganites were successfully described using stretched exponential behaviors,[9] our increasing $\rho(T)$ curves are better described by a logarithmic form, as shown in Fig. 1. Logarithmic time dependences likely originate from a distribution of energy barriers and, as in the case of the relaxation of the magnetization in magnetic nanoparticles, our T^* plays the equivalent role of a blocking temperature for the thermally activated motion of the nanoscopic defects. Pushing further the comparison, the relationship between the characteristic activation energy for the relaxation of the system and the blocking temperature is given by $U \approx \ln(\nu_0 \tau) kT^*$, where $\nu_0 \sim 10^9$ s^{-1} is the relaxation attempt frequency, $\tau \sim 10^3$ s is the characteristic measurement time, and k is the Boltzmann constant. Using $T^* \sim 140$ K for $La_{1/3}Ca_{2/3}MnO_3$ and $Pr_{1/3}Ca_{2/3}MnO_3$, we estimate a typical activation energy $U \sim 0.3$ eV. This value is at an energy scale similar to the hopping energy for the thermally activated motion of polarons in manganites.[25] Then, we speculate that as the defects move through the CO volume they must overcome an energy barrier associated to the lattice distortion of the surrounding CO phase.[12]

In the $La_{0.23}Ca_{0.77}MnO_3$ sample, the increasing resistivity of the CO phase competes against a totally different relaxation mechanism, i.e., the motion of the domain boundaries that separate the CO-orthorhombic domains from the CD-monoclinic ones. These domain boundaries correspond to structural interfaces between regions of different lattice structures; thus they can be directly observed in TEM experiments. Indeed, high-resolution TEM images show that, for temperatures below 135 K ($T/T_{CO} \leq 0.6$), the coexistence of the CO and CD phases becomes dynamic;[2] the CD-monoclinic domains expand and advance over the CO volume. The more delocalized nature of the charge carriers in the CD phase induces the reduction in the overall resistivity of the material ($d\rho/dt < 0$) in the same temperature range. This dynamic coexistence extends down to $T \sim 64$ K (dynamic PS regime in Fig. 2). At this temperature the relaxation rate changes sign and becomes positive again, indicating the freezing of the motion of the domain boundaries. Furthermore, it is remarkable that this change in the dynamic properties coincides with the occurrence of a magnetic transition. As shown by the M-T curves in Fig. 4, at $T_C \sim 64$ K ($T/T_{CO} \sim 0.3$) the sample develops a small FM moment. This behavior denotes the strong coupling between the magnetic and lattice degrees of freedom in this manganite; when the FM component disappears the structural interfaces are allowed to move and the CD-monoclinic volume starts expanding.

In order to disentangle the origin of this FM component, we designed the magnetic relaxation experiment depicted by the sketch shown inside Fig. 4. The maximum negative re-

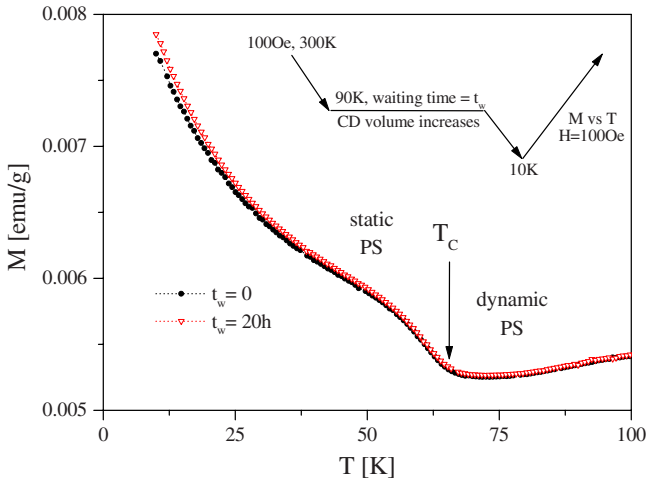

FIG. 4. (Color online) Magnetization vs temperature for $La_{0.23}Ca_{0.77}MnO_3$ measured on warming after cooling using the procedure shown in the sketch (see below). The magnetic transition at $T_C \sim 64$ K triggers a crossover between the static and dynamic phase-separation (PS) regimes. Cooling procedure (follow the direction of the arrows): (1) the sample is cooled from 300 to 90 K at 4 K/min with an applied magnetic field $H=100$ Oe, (2) the sample is kept at 90 K for a period t_w (the waiting time), (3) cooling to 10 K is resumed, and (4) M vs T is measured for different values of t_w, as shown in the main panel.

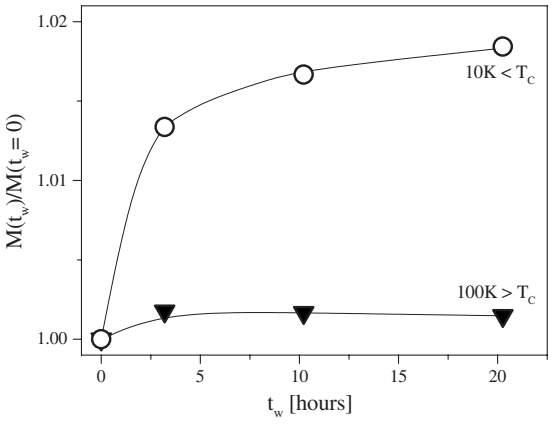

FIG. 5. Magnetic moment of the $La_{0.23}Ca_{0.77}MnO_3$ sample as a function of t_w (the time waited at $T=90$ K during the cooling process, see Fig. 4). For $T=10$ K (lower than $T_C \sim 64$ K) there is a clear increase in the magnetic moment with t_w, as opposed to the case $T=100$ K.

laxation rate of the resistivity is found at 90 K ($T/T_{CO} \sim 0.4$, see Fig. 2). Therefore, we cooled the sample $x=0.77$ from 300 to 90 K at 4 K/min, with an applied magnetic field $H=100$ Oe. The sample was kept at 90 K for different periods of time (the waiting time t_w), during which the phase-separated state was allowed to relax. Then, the cooling process down to 10 K was resumed. Finally we measured the different M vs T curves on warming, as presented in Fig. 4. Since at 90 K the CD volume increases with time, each of these curves corresponds to different amounts of CD-monoclinic phase in the material.

As observed in Fig. 4, for temperatures above T_C there is no significant difference in the magnetization for different t_w, as both the CO and CD phases are AFM and expected to have similar small magnetizations.[2] However, below T_C there is a small but clear increase in the magnetic moment when t_w changes from 0 to 20 h. This behavior is more clearly observed in Fig. 5, where we plot M as a function of t_w at two selected temperatures (these data were taken from the M-T curves like those shown in Fig. 4). At 10 K ($<T_C$), the unambiguous increase in magnetization with t_w indicates that a phase with a larger magnetic moment (the one that develops the FM contribution) is gaining importance as t_w increases. Since it is the CD phase that expands during the waiting time, we conclude that the FM component appearing at $T_C \sim 64$ K must be associated with the presence of the charge-disordered monoclinic domains.

We must note that although it is clearly observed, the magnitude of this FM component is extremely small. Typical FM manganites measured under the same magnetic field (100 Oe) show, at the Curie temperature, magnetization jumps ΔM of the order of 5–15 emu/g.[18,26] However, in $La_{0.23}Ca_{0.77}MnO_3$ the ΔM at $T_C \sim 64$ K is only ~ 0.001 emu/g or less (~ 0.002 emu/g with $H=500$ Oe). This is only a small fraction, $\sim 0.01\%$, of the typical values in FM manganites. Regularly, in other phase-separated manganites where a FM phase coexists with a low-magnetization phase, this fraction could be taken as a measure of the FM volume fraction. However, the TEM images of $La_{0.23}Ca_{0.77}MnO_3$ show that the volume fraction of CD phase responsible for the FM component is well above 0.01%, being around $\sim 20\%$.[2] In fact, neutron-scattering experiments in the similar $La_{1/4}Ca_{3/4}MnO_3$ compound show a 25% volume fraction of the CD-monoclinic phase.[24] We conclude then that the FM moment that appears at T_C could correspond to a slight canting of the spins in the CD-monoclinic volume. The magnetic configuration of this monoclinic phase corresponds to a C-type antiferromagnet,[27] where the charge carriers are confined in one-dimensional straight FM chains. Adjacent chains are compensated, producing a macroscopic AFM order. Then, a weak electronic coupling between these chains may be able to induce a spin canting, giving a small net FM moment.[28] It is also possible that this FM contribution appears at the interfaces between the CD and CO domains. In this case, the small increase in magnetization as a function of t_w would be related to the creation of a few new domain boundaries and/or their expansion during the relaxation process at 90 K. Likely, the FM moment could develop as a result of modified magnetic interactions across the abrupt and strained interfaces between the CO and CD domains.[2] Moreover, the magnetic structure of the CO phase corresponds to antiferromagnetically coupled zigzag FM chains,[21,24] reminiscent of the charge exchange (CE)-type structure typical of half-doped compounds, and different from the C-type structure of the monoclinic regions. The difference in the magnetic structures of these AFM phases could also play role in determining the appearance of a FM moment at the interfaces.

Whichever is the case, it is remarkable that this small FM moment has such a notable effect, freezing the domain boundary dynamics below T_C. It is reasonable to think that a strong magnetoelastic coupling is responsible for this behav-

ior, as already observed in other similar compounds where the CD-monoclinic phase is also present.[27] The CO and CD phases are structurally different, showing different angles between the different structural axes.[2] Therefore the domain boundary motion necessarily implies atom displacements, i.e., strong martensitic strains would be naturally present at the CO/CD interfaces.[3,4,16] The ferromagnetic moment could require specific structural characteristics, especially around these interfaces, such that it becomes energetically unfavorable to change the surrounding lattice with the consequent trapping of the domain boundaries. This interplay between magnetic and structural phases is another feature of the delicate energy balance that dominates the overall physical properties of the manganese perovskites. Of course, the relative influence of this kind of magnetoelastic interactions on the phase stability of phase-separated manganites would compete with several other intrinsic as well as extrinsic factors, such as substrate-induced strain in thin films,[15] sample nanostructuring,[29] grain boundaries,[20] etc. However, it is clear that in our case the magnetic transition plays a crucial role in determining the dynamic properties of the structural phase coexistence.

As the temperature of the $La_{0.23}Ca_{0.77}MnO_3$ sample rises across the magnetic transition at $T_C \sim 64$ K the dynamics of the structural interfaces becomes activated. As a consequence, the competition with the intrinsic relaxation of the CO phase is highlighted and the time evolution of the resistivity shows a distinctive feature. As shown in Fig. 6 for $T=64$ K ($\sim T_C$), $\rho(t)$ shows a positive slope at the beginning of the experiment, indicative of the intrinsic relaxation of the resistivity of the CO phase. However, after approximately 135 min the resistivity reaches a maximum and starts decreasing again, indicating that at long time scales the domain boundary dynamics dominates in the relaxation of the resistivity. This kind of $\rho(t)$ curve was also obtained at 65 K, with the only difference that the domain boundary dynamics (negative slope) becomes dominant after a shorter time of ~ 100 min, as expected. At $T=70$ K the expansion of the CD-monoclinic domains dominates, and the initial increase in resistivity is no longer observed. On the other side of the magnetic transition, at $T=60$ K the structural interfaces are already frozen and $d\rho/dt$ is always positive. This means that the dynamic transition is as sharp as the magnetic transition occurring at T_C, confirming the intimacy between both effects.

In summary, we observe that time relaxation phenomena are common to several electron-doped manganites. However,

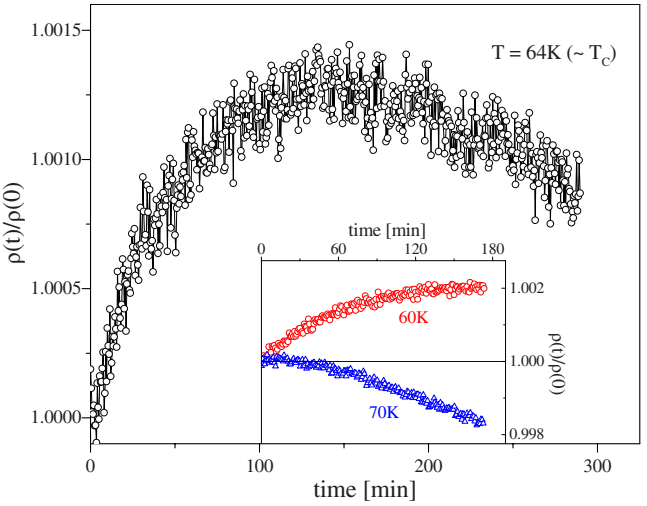

FIG. 6. (Color online) For temperatures close to $T_C \sim 64$ K the temporal evolution of the electrical resistivity of $La_{0.23}Ca_{0.77}MnO_3$ shows a curious peak, related to the competition of two different relaxation mechanisms. Inset: for temperatures at either side of T_C a single relaxation mechanism is observed (ρ increases with time for $T<T_C$ and decreases with time for $T>T_C$).

TEM experiments demonstrate that the microscopic mechanisms of the relaxation can be quite different. On one hand, resistivities increasing with time are observed in several compounds, which can be attributed to a nonperfect charge-ordered phase whose ordering improves with time. On the other hand, the presence of the secondary (charge-disordered) phase in $La_{0.23}Ca_{0.77}MnO_3$ induces a decrease in the resistivity with time through the motion of the CO/CD structural interfaces. Notably, we found that a change in the magnetic moment of the CD phase drives a dynamic transition in the phase-separated state. At this dynamic transition, the competition between the two different resistivity relaxation mechanisms is highlighted. These results reveal a close interplay between magnetic and lattice degrees of freedom (magnetoelasticity) and its large effect on the delicate energy balance of manganite compounds.

J.T. and J.M.Z. were supported by the U.S. Department of Energy under Grant No. DEFG02-01ER45923. Microscopy was carried out at the Center for Microanalysis of Materials at the Frederick Seitz Materials Research Laboratory, which is partially supported by the U.S. Department of Energy under Grant No. DEFG02-91-ER45439.

*Present address: Condensed Matter Physics and Materials Science Department, Brookhaven National Laboratory, Upton, NY 11973, USA.

†Present address: School of Natural Sciences and Mathematics, The University of Texas at Dallas, Richardson, TX 75083, USA.

[1] E. Dagotto *et al.*, Phys. Rep. **344**, 1 (2001); M. B. Salamon and M. Jaime, Rev. Mod. Phys. **73**, 583 (2001); J. M. D. Coey *et al.*, Adv. Phys. **48**, 167 (1999).

[2] J. Tao, D. Niebieskikwiat, M. B. Salamon, and J. M. Zuo, Phys. Rev. Lett. **94**, 147206 (2005).

[3] W. J. Lu, Y. P. Sun, B. C. Zhao, X. B. Zhu, and W. H. Song, Phys. Rev. B **73**, 214409 (2006).

[4] V. Hardy, S. Majumdar, M. R. Lees, D. M. Paul, C. Yaicle, and M. Hervieu, Phys. Rev. B **70**, 104423 (2004); V. Hardy, A. Maignan, S. Hebert, C. Yaicle, C. Martin, M. Hervieu, M. R. Lees, G. Rowlands, D. M. Paul, and B. Raveau, *ibid.* **68**,

220402(R) (2003); R. Mahendiran, A. Maignan, S. Hebert, C. Martin, M. Hervieu, B. Raveau, J. F. Mitchell, and P. Schiffer, Phys. Rev. Lett. **89**, 286602 (2002).

[5] Y. Q. Ma, W. H. Song, R. L. Zhang, J. M. Dai, J. Yang, J. J. Du, Y. P. Sun, C. Z. Bi, Y. J. Ge, and X. G. Qiu, Phys. Rev. B **69**, 134404 (2004).

[6] D. Niebieskikwiat and M. B. Salamon, Phys. Rev. B **72**, 174422 (2005).

[7] Y. Kawasaki, T. Minami, Y. Kishimoto, T. Ohno, K. Zenmyo, H. Kubo, T. Nakajima, and Y. Ueda, Phys. Rev. Lett. **96**, 037202 (2006).

[8] J. Sacanell, F. Parisi, J. C. P. Campoy, and L. Ghivelder, Phys. Rev. B **73**, 014403 (2006); L. Ghivelder and F. Parisi, *ibid.* **71**, 184425 (2005).

[9] M. Matsukawa, K. Akasaka, H. Noto, R. Suryanarayanan, S. Nimori, M. Apostu, A. Revcolevschi, and N. Kobayashi, Phys. Rev. B **72**, 064412 (2005); V. Markovich, G. Jung, Y. Yuzhelevski, G. Gorodetsky, A. Szewczyk, M. Gutowska, D. A. Shulyatev, and Y. M. Mukovskii, *ibid.* **70**, 064414 (2004); P. Levy, F. Parisi, L. Granja, E. Indelicato, and G. Polla, Phys. Rev. Lett. **89**, 137001 (2002).

[10] A. Moreo, M. Mayr, A. Feiguin, S. Yunoki, and E. Dagotto, Phys. Rev. Lett. **84**, 5568 (2000); M. B. Salamon, P. Lin, and S. H. Chun, *ibid.* **88**, 197203 (2002); D. Niebieskikwiat, R. D. Sanchez, A. Caneiro, and B. Alascio, Phys. Rev. B **63**, 212402 (2001).

[11] A. Moreo *et al.*, Science **283**, 2034 (1999); S. Yunoki, J. Hu, A. L. Malvezzi, A. Moreo, N. Furukawa, and E. Dagotto, Phys. Rev. Lett. **80**, 845 (1998); J. Lorenzana, C. Castellani, and C. Di Castro, Phys. Rev. B **64**, 235127 (2001).

[12] K. H. Ahn *et al.*, Nature (London) **428**, 401 (2004); K. H. Ahn, T. Lookman, A. Saxena, and A. R. Bishop, Phys. Rev. B **71**, 212102 (2005).

[13] Note that we retain the term charge ordering in spite of the fact that this strongly insulating phase is more like a charge-density wave. See, for example, S. Cox *et al.*, Nat. Mater. **7**, 25 (2008); J. C. Loudon, S. Cox, A. J. Williams, J. P. Attfield, P. B. Littlewood, P. A. Midgley, and N. D. Mathur, Phys. Rev. Lett. **94**, 097202 (2005), see also Refs. 21 and 22.

[14] M. Uehara and S.-W. Cheong, Europhys. Lett. **52**, 674 (2000); R. Mahendiran, B. Raveau, M. Hervieu, C. Michel, and A. Maignan, Phys. Rev. B **64**, 064424 (2001); C. Yaicle, C. Frontera, J. L. Garcia-Munoz, C. Martin, A. Maignan, G. Andre, F. Bouree, C. Ritter, and I. Margiolaki, *ibid.* **74**, 144406 (2006).

[15] V. Markovich, G. Jung, Y. Yuzhelevskii, G. Gorodetsky, F. X. Hu, and J. Gao, Phys. Rev. B **75**, 104419 (2007); I. C. Infante, F. Sanchez, J. Fontcuberta, M. Wojcik, E. Jedryka, S. Estrade, F. Peiro, J. Arbiol, V. Laukhin, and J. P. Espinos, *ibid.* **76**, 224415 (2007).

[16] P. Littlewood, Nature (London) **399**, 529 (1999); V. Podzorov, B. G. Kim, V. Kiryukhin, M. E. Gershenson, and S. W. Cheong, Phys. Rev. B **64**, 140406(R) (2001); V. Hardy *et al.*, *ibid.* **69**, 020407(R) (2004); P. A. Sharma, S. B. Kim, T. Y. Koo, S. Guha, and S. W. Cheong, *ibid.* **71**, 224416 (2005).

[17] J. Tao and J. M. Zuo, Phys. Rev. B **69**, 180404(R) (2004).

[18] D. Niebieskikwiat, R. D. Sanchez, L. Morales, and B. Maiorov, Phys. Rev. B **66**, 134422 (2002).

[19] J. C. Loudon and P. A. Midgley, Phys. Rev. B **71**, 220408(R) (2005).

[20] P. R. Sagdeo, S. Anwar, and N. P. Lalla, Phys. Rev. B **74**, 214118 (2006).

[21] P. G. Radaelli, D. E. Cox, L. Capogna, S. W. Cheong, and M. Marezio, Phys. Rev. B **59**, 14440 (1999).

[22] R. Wang, J. Gui, Y. Zhu, and A. R. Moodenbaugh, Phys. Rev. B **61**, 11946 (2000).

[23] R. Wang, J. Gui, Y. Zhu, and A. R. Moodenbaugh, Phys. Rev. B **63**, 144106 (2001); M. T. Fernández-Díaz, J. L. Martinez, J. M. Alonso, and E. Herrero, *ibid.* **59**, 1277 (1999).

[24] M. Pissas and G. Kallias, Phys. Rev. B **68**, 134414 (2003).

[25] M. Jaime *et al.*, Appl. Phys. Lett. **68**, 1576 (1996).

[26] D. Niebieskikwiat and R. D. Sánchez, J. Magn. Magn. Mater. **221**, 285 (2000); D. Niebieskikwiat *et al.*, *ibid.* **237**, 241 (2001); L. M. Rodríguez-Martínez and J. P. Attfield, Phys. Rev. B **63**, 024424 (2000); C. Martin, A. Maignan, M. Hervieu, and B. Raveau, *ibid.* **60**, 12191 (1999).

[27] C. D. Ling, E. Granado, J. J. Neumeier, J. W. Lynn, and D. N. Argyriou, Phys. Rev. B **68**, 134439 (2003).

[28] P. G. de Gennes, Phys. Rev. **118**, 141 (1960).

[29] D. Niebieskikwiat, L. E. Hueso, J. A. Borchers, N. D. Mathur, and M. B. Salamon, Phys. Rev. Lett. **99**, 247207 (2007); H. Y. Zhai, J. X. Ma, D. T. Gillaspie, X. G. Zhang, T. Z. Ward, E. W. Plummer, and J. Shen, *ibid.* **97**, 167201 (2006); C. L. Lu *et al.*, Appl. Phys. Lett. **91**, 032502 (2007).